

# An ultra-thin triple-band polarization-insensitive metamaterial absorber for S, C and X band applications

Sameer Kumar Sharma<sup>1</sup> · Saptarshi Ghosh<sup>1</sup>  · Kumar Vaibhav Srivastava<sup>1</sup>

Received: 3 May 2016 / Accepted: 22 November 2016 / Published online: 2 December 2016  
© Springer-Verlag Berlin Heidelberg 2016

**Abstract** In this paper, a polarization-insensitive triple-band metamaterial absorber is proposed for wide angle of incidence. The proposed absorber has been designed in such a way that absorptions occur in S, C and X bands at 3.1, 4.6 and 9.5 GHz, respectively. The unit cell consists of two modified square-shaped closed-loop resonators printed on top of a dielectric substrate and backed by a complete copper lamination. The proposed structure is ultra-thin having a total thickness of 1.6 mm, approximately  $\lambda_0/61$ ,  $\lambda_0/41$  and  $\lambda_0/20$  with respect to absorption frequencies in various bands, where  $\lambda_0$  is the free space wavelength. Moreover, the structure shows good absorptions over wide angle of incidence up to  $45^\circ$  for both TE- and TM-polarized waves. Surface current and electric field distributions have been studied to analyse the absorption mechanism of the proposed absorber. Parametric analyses have also been carried out for suitable selection of absorption frequencies. Finally, a prototype of the absorber has been fabricated and experimentally tested in order to validate the simulation results which are in good agreement.

## 1 Introduction

A lot of research is being carried out in the domain of metamaterials and its electromagnetic applications from the past decade [1–3]. Metamaterials are artificial structures which exhibit exotic properties of controllable medium parameters. These characteristics have allowed them to be used in numerous applications such as cloaking [4], antennas [5], lenses [6] and thermal imaging [7]. Many researchers are also interested in absorber applications at microwave [8, 9], infrared [10] and optical frequencies [11] as well. A perfect absorber is characterized by its simultaneous minimum reflection and transmission capability. The first metamaterial-based absorber was designed by Landy et al. [12] in 2008 and since then several polarization-dependent [13–15], polarization-independent [16, 17], dual-band [18, 19], multi-band [20, 21], large incident angle [22, 23], broadband [24–26] absorbers have been demonstrated by various research groups and have been reported in the literature. Recently, several tunable [27, 28] and switchable [29] absorbers are also developed. Various compact, multi-layered metamaterial absorbers have also been presented with small unit cell sizes, but their utilization is largely restricted by their overall thicknesses [30]. Zhai et al. [31] have presented a dual-band polarization-insensitive metamaterial absorber using Jerusalem cross structure of different sizes. Similarly, Bhattacharya et al. [32] have reported a triple-band metamaterial absorber using electric field driven LC resonators for C band while Ma et al. [33] have presented a triple-band absorber for C, X and Ku band. However, all these structures fail in terms of compactness of unit cell.

In this paper, an ultra-thin polarization-insensitive triple-band absorber has been proposed which can operate in S, C and X bands, respectively. It offers absorption of more

---

✉ Saptarshi Ghosh  
joysaptarshi@gmail.com  
Sameer Kumar Sharma  
sharma.sameer16@gmail.com  
Kumar Vaibhav Srivastava  
kvs@iitk.ac.in

<sup>1</sup> Department of Electrical Engineering, Indian Institute of Technology Kanpur, Kanpur 208016, India

than 76% at all absorption frequencies for wide angle of incidence up to 60° for both TE- and TM-polarized waves. The simulation results show three distinct absorption peaks of 99.67, 97.52 and 99.84% at 3.1, 4.6 and 9.5 GHz, respectively, for normal incidence. Surface current density and electric field distributions have been plotted for understanding the absorption mechanism. Parametric analysis provides detailed analysis for suitable selection of the second and third bands and thus can be ably selected for different application areas. The S-parameter measurements have been carried out in anechoic chamber and are in good agreement with simulation results. Measured peaks occur at 3.18, 4.39 and 9.86 GHz with absorption coefficients of 98.6, 95.6 and 99.1%, respectively, under normal incidence. The proposed absorber is more compact having unit cell dimension ( $\lambda_0/6.5$ ) and thickness ( $\lambda_0/61$ ) at lowest absorption frequency (3.1 GHz) as compared to earlier reported absorbers.

### 2 Structure design and absorbance mechanism

The proposed absorber has been designed on FR4 Epoxy substrate ( $\epsilon_r = 4.25$ ,  $\tan \delta = 0.025$ ) with thickness of 1.6 mm and its unit cell is shown in Fig. 1a with optimized geometrical parameters along with the directions of incident electric field vector ( $E$ ), magnetic field vector ( $H$ ) and electromagnetic wave vector ( $k$ ). The proposed unit cell consists of two modified square-shaped closed-loop resonators (CLRs) printed on top of the dielectric surface while bottom layer is completely backed by copper sheet. The thickness of top and bottom copper layers is 0.017 mm with a conductivity of  $5.8 \times 10^7$  S/m. Figure 1b shows the 3-D perspective view of the unit cell of the proposed structure. The absorption ( $A(\omega)$ ) from the structure can be found out from 1 where  $S_{11}$  is reflection

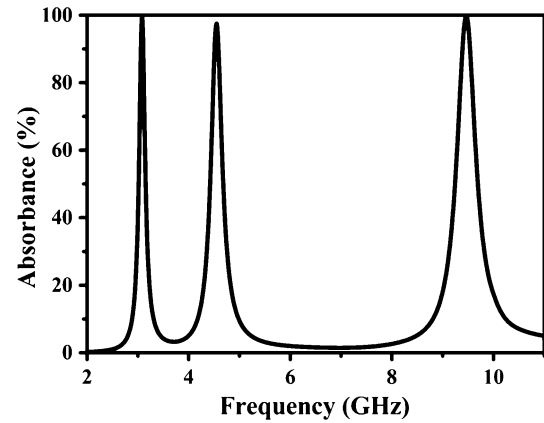


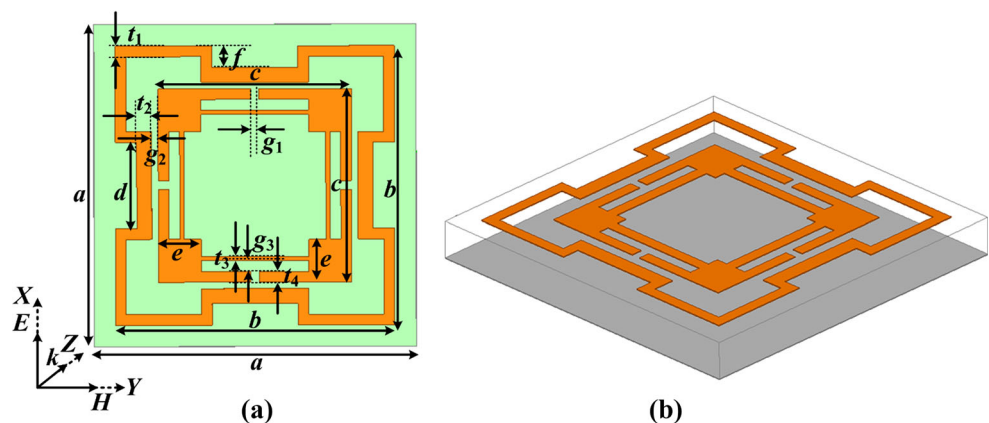
Fig. 2 Simulated absorbance profile of proposed absorber under normal incidence

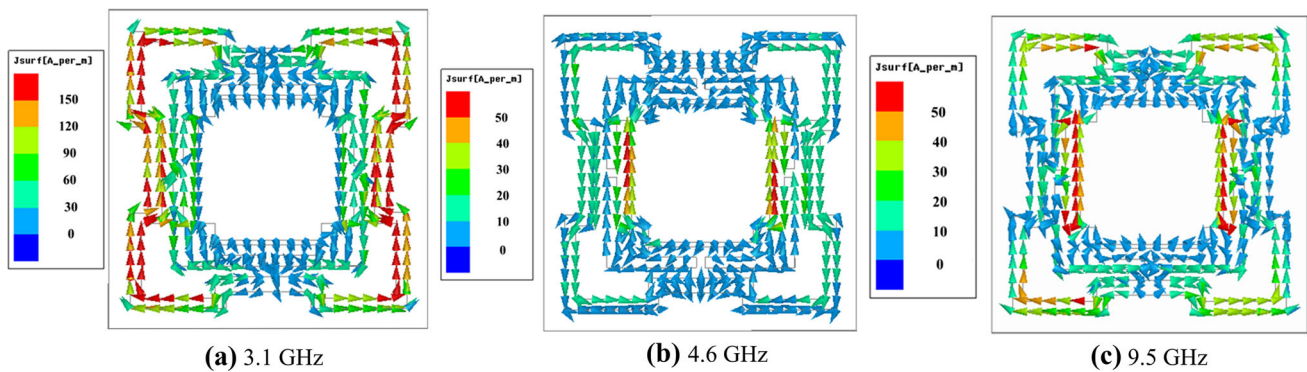
coefficient and  $S_{21}$  is transmission coefficient. The proposed absorber has a copper lamination at the back side which results in zero transmitted power, i.e.  $|S_{21}|^2$  is zero.

$$A(\omega) = 1 - |S_{11}|^2 - |S_{21}|^2 = 1 - |S_{11}|^2 \tag{1}$$

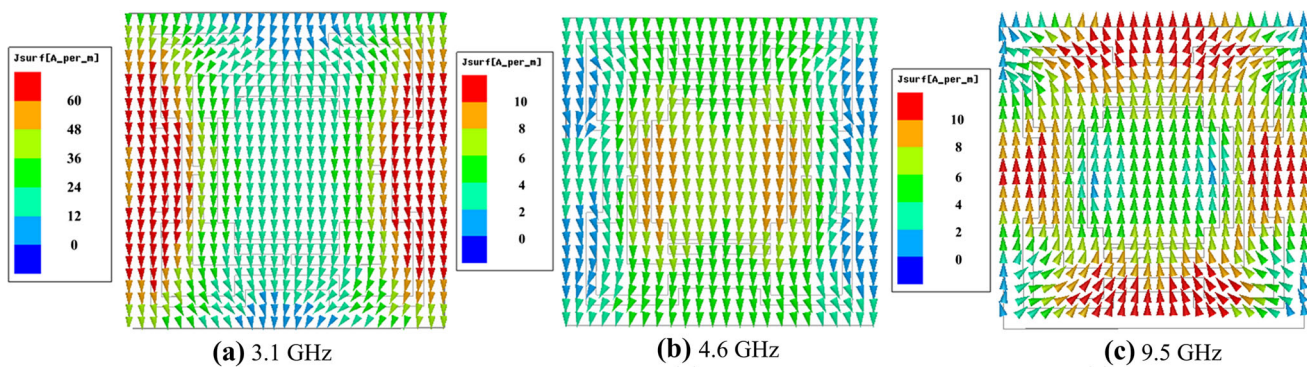
The proposed absorber shows three narrow band absorption peaks at 3.1, 4.6 and 9.5 GHz with absorption of 99.67, 97.52 and 99.84%, respectively, as shown in Fig. 2. The full width half maximum (FWHM) bandwidths of 5.1, 5.6 and 4.7% have also been achieved at these frequencies, respectively. The thickness of proposed structure is approximately  $\lambda_0/61$ ,  $\lambda_0/41$  and  $\lambda_0/20$  with respect to absorption frequencies in various bands with a unit cell dimension of  $\lambda_0/6.5$  at 3.1 GHz. Surface current density profiles have been shown at frequencies with peak absorptions in Figs. 3 and 4 for top and bottom surfaces, respectively, for better understanding of the absorption mechanism. It is seen that currents are mainly concentrated at outer CLR for 3.1 GHz, inner CLR at 4.6 GHz and a combination of both (vertical arms of inner CLR and corners of outer CLR) for 9.5 GHz, respectively. Moreover, the directions of current paths are anti-parallel with respect to ground which results in circulating current loops within the

Fig. 1 Proposed triple-band polarization-insensitive absorber. a Front view of unit cell structure with dimensions:  $a = 15$ ,  $b = 13$ ,  $c = 9$ ,  $d = 4$ ,  $e = 2$ ,  $f = 1$ ,  $t_1 = 0.5$ ,  $t_2 = 0.7$ ,  $t_3 = 0.2$ ,  $t_4 = 0.5$ ,  $g_1 = 0.4$ ,  $g_2 = 0.3$ ,  $g_3 = 0.5$  (unit: mm), and b 3-D perspective view





**Fig. 3** Surface current density on top layer of proposed absorber at respective absorption frequencies



**Fig. 4** Surface current density on bottom layer of proposed absorber at respective absorption frequencies

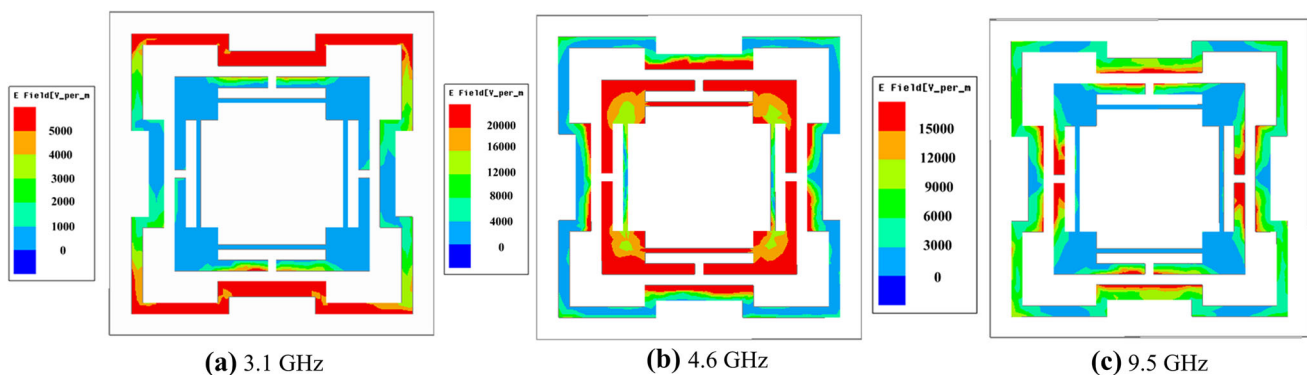


**Fig. 5** Electric field distribution on top layer of proposed absorber at respective absorption frequencies

structure. This current direction is perpendicular to the incident magnetic field which further leads to magnetic excitation. This magnetic excitation is responsible for controlling the effective permeability.

Figure 5 shows the concentration of induced electric fields distributions at top surface of proposed absorber for absorption frequencies 3.1, 4.5 and 9.5 GHz, respectively. These electric fields control the electric excitation which in turn controls the effective permittivity. Outer CLR provides larger electrical path for current to traverse while

inner CLR has shorter electrical length due to dimensions. At resonance frequencies, both the electric and magnetic resonances become significant and high absorption is realized. Therefore, the absorptions of the proposed structure are resulted due to simultaneous excitation of electric and magnetic mode.

In order to explain the contribution of the individual element in the absorption response, different parts of the structure is simulated separately. Initially a Minkowski fractal-based square loop is chosen, which is modified at

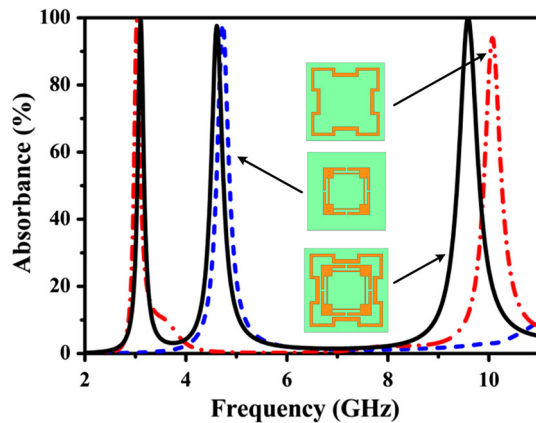


**Fig. 6** Contribution of individual element in the absorbance response while designing the proposed structure

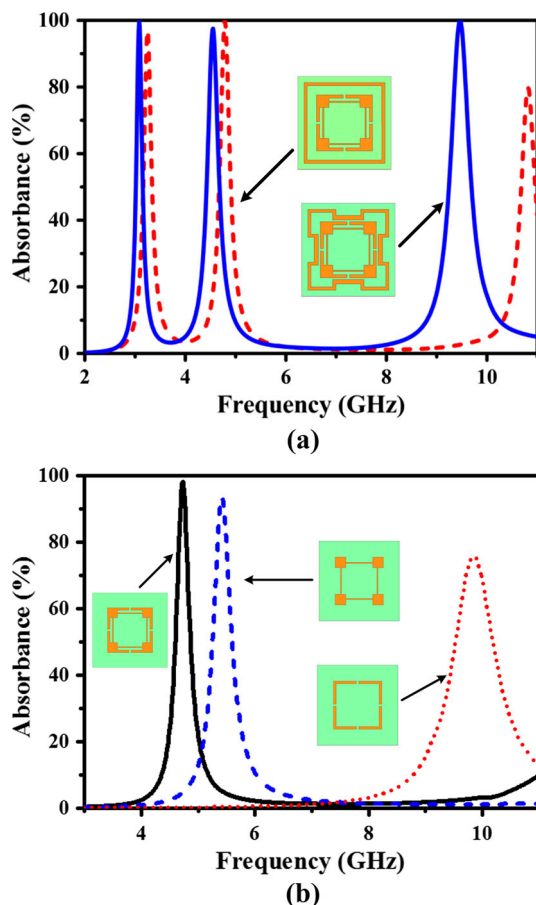


**Fig. 7** **a** Contribution of Minkowski fractal instead of simple square loop and **b** contribution of individual element of the inner geometry in the absorption response of the proposed structure

the corners to increase the electrical length. It shows two resonances at S and X band. Then a modified split ring resonator has been designed to operate at C band. Finally, both of these resonating structures are combined together to obtain three resonances as shown in Fig. 6.

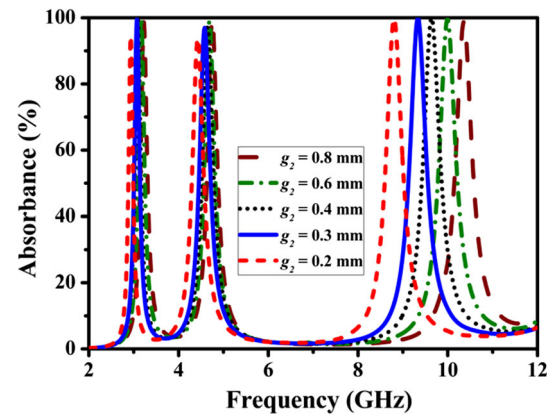


**Fig. 8** Variation in absorbance of proposed absorber with change in gap  $g_2$

We have also shown the design methodology of selecting Minkowski fractal instead of simple square loop in Fig. 7a. It is observed that the fractal geometry has higher electrical length, which reduces the absorption frequencies and makes the unit cell compact. The inner geometry consists of two elements—a capacitive and an inductive square loop. Both the square loops exhibit narrow band absorbance in high-frequency range separately but, while combined together, result in a lower absorption frequency in C band as shown in Fig. 7b.

Parametric analyses have been carried out on critical parameters in order to converge at proposed design. Figure 8 shows the variation in absorption frequency by changing the gap  $g_2$ . It is seen that by decreasing  $g_2$ , effective capacitance between outer and inner CLR increases which lowers the absorption frequency of the third band while the first and second band are almost unaffected. It is due to the fact that the first and second bands are due to loops formed by outer CLR and inner CLR as shown earlier in Figs. 4 and 5, and thus, capacitive coupling between these loops does not play any significant role in deciding absorption frequency for these bands. Frequency of the second band can be suitably selected by varying the width  $t_3$  of inner loop which is as shown in Fig. 9. Absorption frequency can be varied from 4.5 to 5.6 GHz with an absorption peak greater than 80% for variation in width from 0.2 to 2 mm, respectively. As width increases, net inductance offered by the loop decreases which shifts the frequency towards right in frequency spectrum.

### 3 Experimental verification

The proposed triple-band ultra-thin absorber structure has been fabricated on 1.6-mm-thick FR4 epoxy substrate. The fabricated prototype consists of 225 mm  $\times$  225 mm square sample corresponding to 15  $\times$  15 unit cells and is

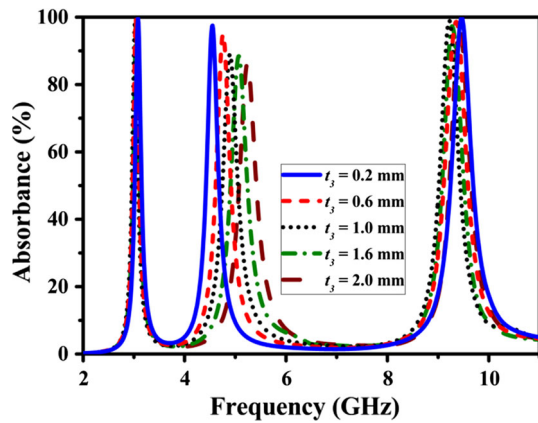


**Fig. 9** Variation in absorbance of proposed absorber with change in width  $t_3$

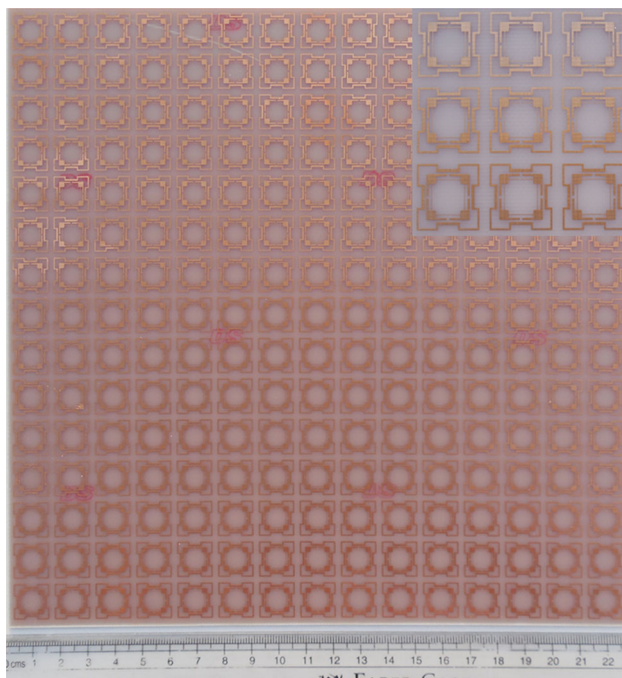
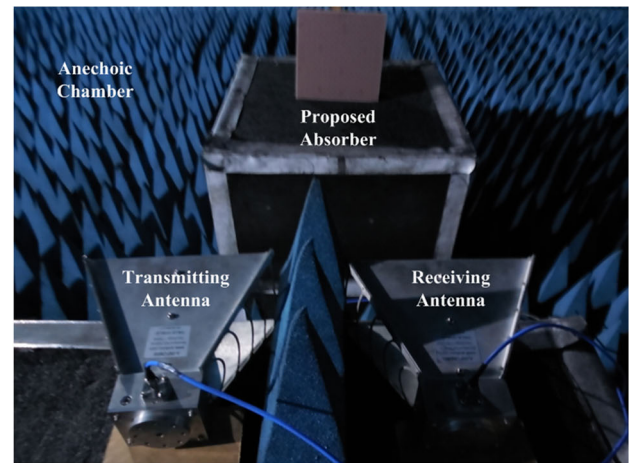
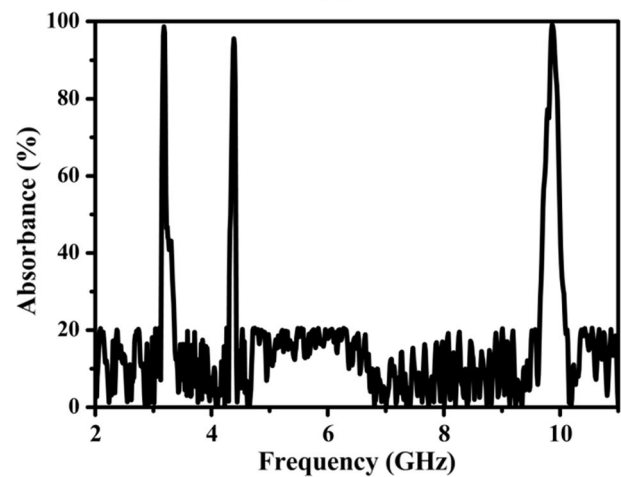


**Fig. 10** Photograph of top layer of fabricated prototype with enlarged view at the *inset*

shown in Fig. 10. Figure 11a shows the measurement set-up for measuring the reflected power along with measured absorbance profile of proposed absorber. Two identical broadband horn antennas (LB-10180-SF) operating in 1–18 GHz are used as a transmitter and receiver for measuring the reflected power coming from the fabricated structure. The experiment has been performed in anechoic chamber, and reflected power has been measured using vector network analyser Agilent N5320A [31]. Initially, a copper plate having identical dimensions as that of the proposed absorber is placed and reflected power is measured over the complete frequency range. The copper plate acts as an ideal reflector and power received at the receiving antenna is



(a)



(b)

**Fig. 11** **a** Experimental set-up to measure reflected power within the anechoic chamber and **b** measured absorbance profile of fabricated structure

smaller than the incident power due to scattering and path loss. Thereafter, similar experiment is performed by replacing copper plate with the proposed absorber. The reflected power from the structure is normalized with respect to the power received from the copper plate. This cancels out the scattering and path loss. Figure 11b shows triple-band response with absorption peaks of 98.6, 95.6 and 99.1% at 3.18, 4.39 and 9.86 GHz, respectively, under normal incidence with full width half maximum (FWHM) bandwidths of 2.5, 2.3 and 3%. The deviation in frequency is due to fabrication tolerances.

The structure has also been studied under normal incidence for different polarization angles as well as under oblique incidence for TE- and TM-polarized waves. Figure 12 displays the simulated and measured response of proposed triple-band absorber for various polarization angles. It is seen that proposed structure is insensitive towards variations in polarization angle and thus can be

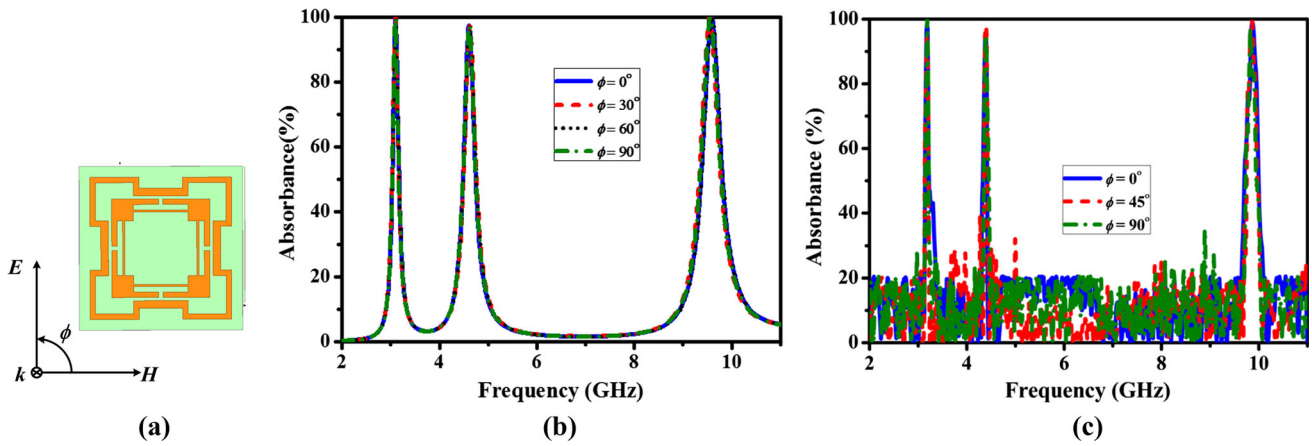


**Fig. 12** **a** Arrangement of the structure for variation in polarization angle, **b** simulated and **c** measured absorption responses of proposed absorber under various polarization angles ( $\phi$ : polarization angle)

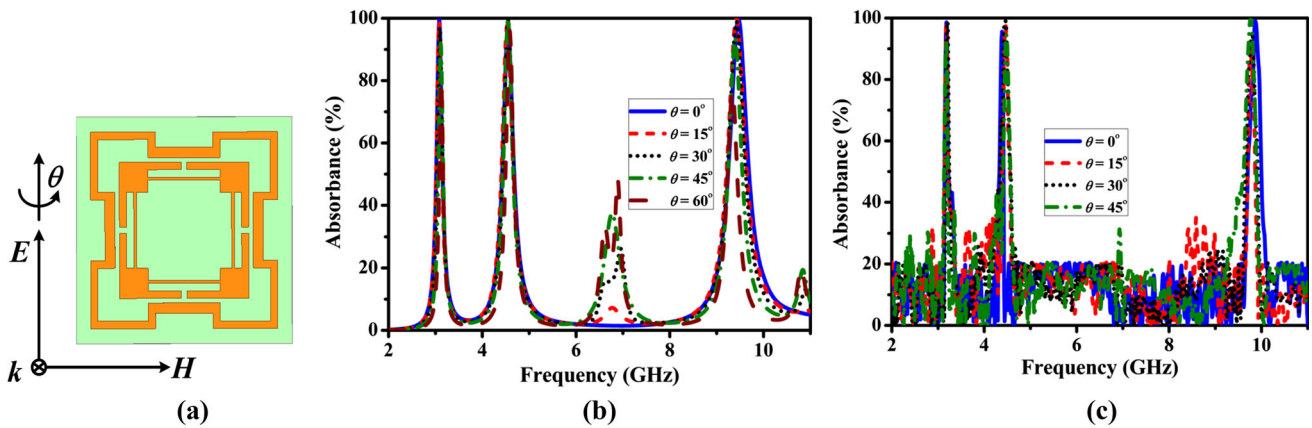


**Fig. 13** **a** Arrangement of the structure for variation in incident angle for TE-polarized wave, **b** simulated and **c** measured absorption responses of proposed absorber under various incident angles for TE-polarized wave ( $\theta$ : incident angle)

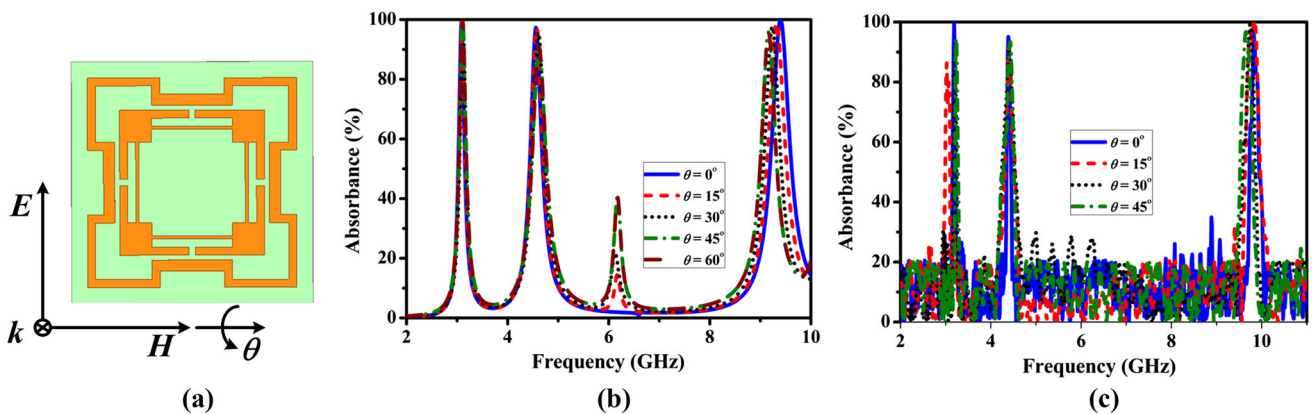


**Fig. 14** **a** Arrangement of the structure for variation in incident angle for TM-polarized wave, **b** simulated and **c** measured absorption responses of proposed absorber under various incident angles for TM-polarized wave ( $\theta$ : incident angle)

practically utilized in numerous applications. Performance of proposed absorber under oblique incidence for TE-polarized wave is shown in Fig. 13. It is seen that the triple-

band response is maintained up to incidence angle of  $45^\circ$  for both simulation and measured results. A small spurious band with very low absorption peak (less than 40%) is seen

**Table 1** Comparison of proposed absorber with earlier published absorbers

References	Electrical size (At lowest absorption freq.)	Thickness (At lowest absorption freq.)	Polarization Insensitive
[30]	$\lambda_0/2.7 \times \lambda_0/2.7$	$\lambda_0/63$	Yes
[32]	$\lambda_0/1.6 \times \lambda_0/1.6$	$\lambda_0/48$	Yes
[33]	$\lambda_0/5.8 \times \lambda_0/5.8$	$\lambda_0/77$	No
Proposed work	$\lambda_0/6.5 \times \lambda_0/6.5$	$\lambda_0/61$	Yes

at 6.8 GHz at higher incidence angles which is due to cross-coupling between the two resonating loops. Figure 14 shows the absorption profile of proposed absorber under oblique incidence for TM-polarized wave. A spurious band at 6.2 GHz is also visible with low absorption peak (less than 40%) which is due to cross-coupling between CLRs. Experimental results are in good agreement with the simulated results for both TE and TM polarizations.

#### 4 Conclusion

An ultra-thin triple-band metamaterial absorber has been presented for S, C and X band applications. The proposed absorber shows excellent performance under oblique incidence for both TE- and TM-polarized wave with absorption peaks greater than 76% for wider angles as well. Also, the structure is polarization insensitive as it is geometrically symmetrical. Parametric behaviour has been studied on vital parameters for suitable selection of the second and third bands. It is ultra-thin with thickness of  $\lambda/61$  and small unit cell dimension of  $\lambda/6.5$ . The proposed absorber has also been compared with earlier reported structures in terms of compactness, miniaturization and sensitivity towards polarization angle which is clearly given in Table 1. The proposed absorber is suitable for radar cross section (RCS) reduction and electromagnetic shielding in various applications such as surveillance, airborne and non-military radiolocation radars.

**Acknowledgements** We would like to thank the staff members of PCB fabrication Laboratory, Department of Electrical Engineering, Indian Institute of Technology Kanpur, for fabricating the structure. This project is partially funded by Indian Space Research Organization (ISRO), India, under Project No. SPO/STC/EE/2014087.

#### References

1. C. Caloz, T. Itoh, *Electromagnetic Metamaterials: Transmission Line Approach and Microwave Applications* (IEEE-Wiley Press, New York, 2005)
2. D.R. Smith, W.J. Padilla, D.C. Vier, S.C. Nemat-Nasser, S. Schultz, Composite medium with simultaneously negative permeability and permittivity. *Phys. Rev. Lett.* **84**(18), 41844187 (2000)

3. R. Marques, F. Martin, M. Sorolla, *Metamaterials with Negative Parameters: Theory, Design and Microwave Applications* (Wiley, Hoboken, 2008)
4. S.A. Cummer, B.I. Popa, D. Schurig, D.R. Smith, J.B. Pendry, Full wave simulations of electromagnetic cloaking structures. *Phys. Rev. E* **74**, 036621 (2006)
5. S.K. Sharma, A. Gupta, R.K. Chaudhary, Epsilon negative CPW-fed zeroth-order resonating antenna with backed ground plane for bandwidth enhancement and miniaturization. *IEEE Trans. Antennas Propag.* **63**(11), 5197–5203 (2015)
6. N. Fang, H. Lee, C. Sun, X. Zhang, Sub-diffraction-limited optical imaging with a silver superlens. *Science* **308**(5721), 534537 (2005)
7. X. Liu, T. Tyler, T. Starr, A.F. Starr, N.M. Jokrest, W.J. Padilla, Taming the blackbody with infrared metamaterials as selective thermal emitters. *Phys. Rev. Lett.* **107**, 045901 (2011)
8. S. Ghosh, S. Bhattacharya, Y. Kaiprath, K.V. Srivastava, Bandwidth-enhanced polarization insensitive microwave metamaterial absorber and its equivalent circuit model. *J. Appl. Phys.* **115**, 104503 (2014)
9. L. Yao, M. Li, X. Zhai, H. Wang, J. Dong, On the miniaturization of polarization insensitive wide angle metamaterial absorber. *Appl. Phys. A* **122**, 61 (2016)
10. N. Zhang, P. Zhou, D. Cheng, X. Weng, J. Xie, L. Deng, Dual-band absorption of mid-infrared metamaterial absorber based on distinct dielectric spacing layers. *Opt. Lett.* **38**(7), 1125–1127 (2013)
11. T. Cao, C.W. Wei, R.E. Simpson, L. Zhang, M.J. Cryan, Fast tuning of double fano resonance using a phase-change metamaterial under low power intensity. *Sci. Rep.* **4**(4463), 19 (2014)
12. N.I. Landy, S. Sajuyigbe, J.J. Mock, D.R. Smith, W.J. Padilla, Perfect metamaterial absorber. *Phys. Rev. Lett.* **100**, 207402 (2008)
13. S. Bhattacharya, S. Ghosh, K.V. Srivastava, Bandwidth enhanced metamaterial absorber using electric field driven LC Resonator for airborne radar applications. *Microw. Opt. Technol. Lett.* **55**(9), 21312137 (2013)
14. B. Wang, S. Liu, B. Bian, Z. Mao, X. Liu, B. Ma, L. Chen, A novel ultrathin and broadband microwave metamaterial absorber. *J. Appl. Phys.* **116**, 094504 (2014)
15. Y. Fan, Z. Wei, Z. Zhang, H. Li, Enhancing infrared extinction and absorption in a monolayer graphene sheet by harvesting the electric dipolar mode of split ring resonators. *Opt. Lett.* **38**(24), 5410–5413 (2013)
16. S. Ghosh, S. Bhattacharya, K.V. Srivastava, Bandwidth enhancement of an ultra-thin polarization insensitive metamaterial absorber. *Microw. Opt. Technol. Lett.* **56**(2), 350355 (2014)
17. Y. Cheng, H. Yang, Z. Cheng, N. Wu, Perfect metamaterial absorber based on a split-ring-cross resonator. *Appl. Phys. A* **102**(1), 99–103 (2011)
18. Y.J. Yoo, Y.J. Kim, P.V. Tuong, J.V. Rhee, K.W. Kim, W.H. Jang, Y.H. Kim, H. Cheong, Y.P. Lee, Polarization-independent dual-band perfect absorber utilizing multiple magnetic resonances. *Opt. Express* **21**(26), 32484–32490 (2013)

19. Y. Zhao, Q. Hao, Y. Ma, M. Lu, B. Zhang, M. Lapsley, I.-C. Khoo, T.J. Huang, Light-driven tunable dual-band plasmonic absorber using liquid-crystal-coated asymmetric nanodisk array. *Appl. Phys. Lett.* **100**, 053119 (2012)
20. X. Huang, H. Yang, S. Yu, J. Wang, M. Li, Triple-band polarization-insensitive wide-angle ultra-thin planar spiral metamaterial absorber. *J. Appl. Phys.* **113**, 213516 (2013)
21. D. Chaurasiya, S. Ghosh, S. Bhattacharya, K.V. Srivastava, An ultrathin quad-band polarization-insensitive wide Angle metamaterial absorber. *Microw. Opt. Technol. Lett.* **57**(3), 697–702 (2015)
22. B. Zhu, Z. Wang, C. Huang, Y. Feng, J. Zhao, T. Jiang, Polarization insensitive metamaterial absorber with wide incident angle. *Prog. Electromagn. Res.* **101**, 231–239 (2010)
23. B. Zhu, Z.B. Wang, Z.Z. Yu, Q. Zhang, J.M. Zhao, Y.J. Feng, T. Jiang, *Chin. Phys. Lett.* **26**, 1141021 (2009)
24. A. Kazemzadeh, A. Karlsson, Multilayered wideband absorbers for oblique angle of incidence. *IEEE Trans. Antennas Propag.* **58**(11), 3637–3646 (2010)
25. P. Munaga, S. Ghosh, S. Bhattacharya, K.V. Srivastava, A fractal-based compact broadband polarization insensitive metamaterial absorber using lumped resistors. *Microw. Opt. Technol. Lett.* **58**(2), 343–347 (2016)
26. X. Zhang, Y. Fan, L. Qi, H. Li, Broadband plasmonic metamaterial absorber with fish-scale structure at visible frequencies. *Opt. Mater. Express* **6**(7), 2448–2457 (2016)
27. F. Zhang, S. Feng, K. Qiu, Z. Liu, Y. Fan, W. Zhang, Q. Zhao, J. Zhou, Mechanically stretchable and tunable metamaterial absorber. *Appl. Phys. Lett.* **106**, 091907 (2015)
28. Y. Fan, N.-H. Shen, T. Koschny, C.M. Soukoulis, Tunable terahertz meta-surface with graphene cut-wires. *ACS Photonics* **2**, 151–156 (2015)
29. S. Ghosh, K.V. Srivastava, Polarization-insensitive single- and broadband switchable absorber/reflector and its realization using a novel biasing technique. *IEEE Trans. Antennas Propag.* **64**(8), 3665–3670 (2016)
30. J.A. Bossard, L. Lin, S. Yun, L. Liu, D.H. Werner, T.S. Meyer, Near-ideal optical metamaterial absorbers with super-octave bandwidth. *ACS Nano* **8**(2), 1517–1524 (2014)
31. H. Zhai, Z. Li, L. Li, C. Liang, A dual-band wide-angle polarization-insensitive ultrathin gigahertz metamaterial absorber. *Microw. Opt. Technol. Lett.* **55**(7), 1606–1609 (2013)
32. S. Bhattacharya, S. Ghosh, D. Chaurasiya, K.V. Srivastava, Bandwidth-enhanced dual-band dual-layer polarization-independent ultra-thin metamaterial absorber. *Appl. Phys. A* **118**, 207–215 (2015)
33. B. Ma, S. Liu, B. Bian, X. Kong, H. Zhang, Z. Mao, B. Wang, Novel three-band microwave metamaterial absorber. *J. Electromagn. Wave Appl.* **28**(12), 1478–1486 (2014)